Frustrated Liquid Crystals: Synthesis and Mesomorphic Behavior of Unsymmetrical Dimers Possessing Chiral and Fluorescent Entities

Channabasaveshwar V. Yelamaggad,*,† Nilesh L. Bonde,§ Ammathnadu S. Achalkumar,† Doddamane S. Shankar Rao,† Subbarao Krishna Prasad,† and Ashish K. Prajapati§

Centre for Liquid Crystal Research, Jalahalli, Bangalore 560 013, India, and Applied Chemistry Department, Faculty of Technology and Engineering, Kalabhavan, P.O. Box No. 51, The M. S. University of Baroda, Vadodara, India

Received October 31, 2006. Revised Manuscript Received March 16, 2007

A novel approach to designing liquid crystal dimers with high chirality is described. The synthesis, and liquid crystal properties of several new optically active unsymmetrical fluorescent dimers belonging to four homologous series are presented. These new oligomesogens possess pro-mesogenic cholesterol as a chiral moiety covalently linked to a fluorescent bent aromatic (chalcone) core through a trimethylene (4-oxybutanoyl)/tetramethylene (5-oxypentanoyl)/pentamethylene (6-oxyhexanoyl)/heptamethylene (8-oxyoctanoyl) central spacer giving rise to four series of chiral dimers. In each series, the chalcone entity is substituted with ethoxy, *n*-butyloxy to *n*-dodecyloxy tails, with the aim of learning the relation between the molecular structure and thermotropic behavior. The molecular structures have been characterized by routine characterization techniques. These compounds are fluorescent, as evidenced by recording the emission spectra for two different excitation maxima for some representative compounds. The mesomorphic properties of these dimers have been evaluated by polarizing microscopic and calorimetric studies; for some representative samples, the X-ray diffraction studies has also been carried additionally. Except one, all other compounds exhibit liquid crystal behavior. Within the homologous series comprising trimethylene, pentamethylene, and heptamethylene central spacer, compounds with short hydrocarbon tails exhibit chiral nematic phase and blue phase, whereas the members with intermediate spacer length (but for few exceptions) show the twist grain boundary and/or smectic A phase/s in addition. The thermal behavior of the higher members of these series seems to be dependent on the length of the central spacer. A similar trend was observed for lower and higher homologues of dimers possessing tetramethylene (5-oxypentanoyl, C5, i.e., odd spacer) spacer. Interestingly, the higher homologues of this series were found to exhibit two twist grain boundary phases consecutively, occurring over a relatively wide thermal range with a new phase sequence. Thus, the occurrence of a fluid frustrated phase, in particular, the blue phase in the majority of the dimers, indicates that chirality of these mesogens is high enough such that the helical pitch of the chiral nematic phase is sufficiently short. This behavior can be attributed to the presence of the bent-core chalcone entity in the dimer structure, which enhances the biaxiality and chirality of the system.

Introduction

The chiral anisotropic fluid phases formed by chiral mesogens or induced by a chiral dopant dissolved in an achiral mesophase have continued to attract special attention ever since their discovery.[1] Such a fascination originates from the fact that these fluid phases are remarkable from both fundamental research and practical application viewpoints.[2,3] For example, the intrinsic chiral bulk properties such as helical structures of the chiral nematic (N*) or chiral smectic C (SmC*) of optically active mesogens have been very well exploited in thermochromic[4] and electro-optic devices respectively.[5] For the orthogonal layered phase, the chiral smectic A (SmA) phase formed by chiral mesogens exhibit the so-called electroclinic effect under the influence of an electrical field that is promising in spatial light modulation applications.[6] The frustrated fluid structures viz., blue phases,[2,4−6] and twist grain boundary (TGB) phases[2] are mainly of scientific curiosity. Three distinct blue phases, namely, blue phase I (BPI), blue phase II (BPII), and blue phase III (BPIII), are known to occur over a very narrow thermal range of a few degrees Celsius between the isotropic (I) phase and N* or smectic (Sm) phases of highly chiral mesogens, where the low-temperature N* phase is character-

* Corresponding author. Tel: 91-80-28381119. Fax: 91-80-28382044. E-mail: Yelamaggad@yahoo.mail.com.
† Centre for Liquid Crystal Research.
§ The M. S. University of Baroda.

(1) Renitzer, F. *Monatsch. Chem.* **1888**, *9*, 421.
(2) Goodby, J. W. In *Hand Book of Liquid Crystals*; Demus, D., Goodby, J. W., Gray, G. W., Spiess, H.-W., Eds.; Wiley-VCH: Weinheim, Germany, 1998; Vol. 1, Chapter V, p 115.
(3) Kitzerow, H. In *Chirality in Liquid Crystals*; Kitzerow, H. -S., Bahr, C. Eds.; Springer-Verlag: New York, 2001.
(4) Sage, I. In *Liquid Crystals*: *Applications and Uses*; Bahadur, B., Ed; World Scientific: Singapore, 1992; Vol. 3, Chapter 20.
(5) (a) Lagerwall, S. T. In *Ferroelectric and Antiferroelectric Liquid Crystals*; Lagerwall, S. T., Ed; Wiley-VCH: Weinheim, Germany, 1999. (b) Walba, D. M. *Science* **1995**, *270*, 250.
(6) (a) Garoff, S.; Meyer, R. *Rev. Lett.* **1977**, *38*, 848. (b) Lagerwall, S. T.; Matuszcyk, M.; Rodhe, P.; Odma, L. In *The Optics of Thermotropic Liquid Crystals*; Elston, S. J., Sambles, J. R., Eds.; Taylor and Francis: London, 1998.

10.1021/cm0625880 CCC: $37.00
Published on Web 04/20/2007

ized by a pitch (P) well below 1 μm with the wavelength of selective reflection in the visible range of the spectrum.[7−12] Among these, BPI and BPII have cubic symmetry, whereas in the BPIII phase, the orientational order of molecules is not periodic and the symmetry is the same as that of the isotropic phase. Recently, bent-core mesogens, either in their pure form or as mixtures, have been engaged as a new molecular design to account for the biaxiality[11] and enhancement of chirality[12] that has resulted in the stabilization of blue phases. Bent-core U-shaped molecules[11] derived from the binaphthyl entity have been demonstrated to exhibit the blue phase in a relatively wide thermal range, the occurrence of which is believed to be a consequence of coupling between the axial chirality of the binaphthyl group and the twist configuration of the two mesogenic segments attached.[11] Interestingly, it has been shown that BPs are induced by doping chiral nematic liquid crystals with achiral bent-core systems.[12]

The TGB phases, as mentioned earlier, are another kind of frustrated phases,[13−19] generally found at the phase transition from the I or N* to SmA or SmC* phases over a narrow temperature interval of a few degrees Celsius. Like the blue phases, they can be observed only in chiral systems with high enantiomeric excess and strong molecular chirality (short pitch). The frustration in these phases originates from an antagonistic situation in which the molecules try to form a helical structure with the chiral nematic helix axis perpendicular to the long axes of the molecules and at the same time their tendency to form a lamellar structure. These two structures are incompatible and cannot coexist. However, the coexistence is attained by having small blocks (sheets) of molecules with a local smectic structure that are rotated with respect to one another through sets of screw dislocations situated at their interface, thereby giving a helical structure. Three types of TGB phases, namely, TGBA, TGBC, and TGBC*, were theoretically predicted in which the smectic structure is orthogonal SmA, tilted SmC, and helical SmC*, respectively. The first experimental confirmation for the occurrence of the TGBA phase was made by Goodby and co-workers in a series of biphenylyl esters of the 4-*n*-alkoxyphenyl-propiolic acids exhibiting the I−TGBA−SmC* phase sequence.[17a,b] Since then, many new molecular systems showing the TGBA phase in different sequences such as I−BP−TGBA, I−TGBA−SmA−SmC*, I−BP−N*−TGBA, I−N*−TGBA−TGBC*, I−N*−TGBA−SmC*, I−BP−N*−TGBC−SmC*, I−BP−N*−TGBA−SmA−SmC*−SmX, I−BPIII−BPII−BP−I−TGBA−TGBC−SmC*, etc., have been reported.[3] Initially, it appeared that chiral systems with a fairly long molecular core viz., three aromatic rings connected axially, is conducive for the stabilization of TGBA phase.[18] However, it was later found that optically active molecules with short molecular axes could also form the TGBA phase.[19] Despite the fact that many conventional (over 3000) monomeric liquid crystals consisting of cholesteryl ester unit as a chiral part of the molecule have been reported, there are only a few cholesterol-based mesogens exhibiting the TGBA or related phases.[20,21] On the other hand, cholesterol-based oligomesogens, in particular dimers, seem to be favorable systems for the stabilization of the frustrated phases, as discussed below.

In recent years, liquid crystal dimers possessing two structurally identical (symmetrical) or different (unsymmetrical) mesogenic cores tied axially through a flexible paraffinic spacer are being investigated intensively[22] not only because they can be regarded as model compounds for polymeric liquid crystals[23] but also because they exhibit fascinating thermal behavior. In particular, unsymmetrical dimers consisting of a cholesteryl ester core as the chiral entity joined to different aromatic mesogens through an alkylene spacer show frustrated phases and interesting sequences.[24−26] For example, the occurrence of a reentrant incommensurate smectic A (SmA_{ic}) and SmC* mesophases in an unsymmetrical dimer formed by joining cholesteryl ester moiety to a Schiff's base through a pentamethylene spacer[24a] has been reported. Studies on a similar type of compounds showed that the length of the spacer and the molecular structure of the non-cholesteryl mesogenic (aromatic) segment is more important for the occurrence of an

(7) Coates, D.; Gray, G. W. *Phys. Lett*. **1973**, *45A*, 115.
(8) Crooker, P. P. *Mol. Cryst. Liq. Cryst*. **1983**, *98*, 31. Crooker, P. P. *Liq. Cryst*. **1989**, *5*, 751.
(9) Right, D. C.; Mermin, N. D. *Rev. Mod. Phys*. **1989**, *61*, 385.
(10) Crooker, P. P. In *Chirality in Liquid Crystals*; Kitzerow, H.-S., Bahr, C., Eds.; Springer-Verlag: New York, 2001; Chapter 7, p 186.
(11) Rokunohe, J.; Yoshizawa, A. *J. Mater. Chem.* **2005**, *15*, 275.
(12) Nakata, M.; Takanishi, Y.; Watanabe, J.; Takezoe, H. *Phy. Rev. E* **2003**, *68*, 041710.
(13) (a) Goodby, J. W. *Curr. Opin. Colloid Interface Sci*. **2002**, *7*, 326. (b) Goodby, J. W.; Nishiyama, I.; Slaney, A. J.; Booth, C. J.; Toyne, K. J. *Mol. Cryst. Liq. Cryst*. **1993**, *14*, 37.
(14) Renn, S. R.; Lubensky, T. C. *Phys. Rev. A* **1988**, *38*, 2132.
(15) Renn, S. R.; Lubensky, T. C. *Mol. Cryst. Liq. Cryst*. **1991**, *209*, 349.
(16) Renn, S. R. *Phys. Rev. A* **1992**, *45*, 953.
(17) (a) Goodby, J. W.; Waugh, M. A.; Stein, S. M.; Chin, E.; Pindak, R.; Patel, J. S. *Nature* **1989**, *337*, 449. (b) Goodby, J. W.; Waugh, M. A.; Stein, S. M.; Chin, E.; Pindak, R.; Patel, J. S. *J. Am. Chem. Soc*. **1989**, *111*, 8119. (c) Goodby, J. W. In *Structure and Bonding*: *Liquid Crystal II*; Mingos, D. M. P., Ed.; Springer-Verlag: Berlin, 1999; p 83.
(18) Goodby, J. W.; Slaney, A. J.; Booth, C. J.; Nishiyama, I.; Vuijk, J. D.; Styring, P.; Toyne, K. J. *Mol. Cryst. Liq. Cryst*. **1994**, *243*, 231.
(19) Nguyen, H. T.; Bouchta, A.; Navailles, L.; Barois, P.; Isaert, N.; Twieg, R. J.; Maaroufi, A.; Destrade, C. *J. Phys. France II* **1992**, *2*, 1889.
(20) (a) Galatina, A. I.; Novikova, N. S.; Derkach, L. G.; Kramarenko, N. L.; Tsyguleva, O. M.; Kuzin, V. F. *Mol. Cryst. Liq. Cryst.* **1986**, *140*, 11. (b) Harwood, S. M.; Toyne, K. J.; Goodby, J. W. *Liq. Cryst*. **2000**, *27*, 443.
(21) (a) Subashree, S.; Sadashiva, B. K. *Curr. Sci*. **2003**, *85*, 1061. (b) Subashree, S.; Sadashiva, B. K. *Liq. Cryst.* **2004**, *31*, 81. (c) Sadashiva, B. K. *Pramana* **1999**, *53*, 213.
(22) (a) Imrie, C. T.; Henderson, P. A. *Curr. Opin. Colloid Interface Sci*. **2002**, *7*, 298. (b) Imrie, C. T. In *Structure and Bonding: Liquid Crystals II*; Mingos, D. M. P., Ed.; Springer-Verlag: Berlin, 1999; p 149.
(23) Griffin, A. C.; Britt, B. R. *J. Am. Chem. Soc*. **1981**, *103*, 4957.
(24) (a) Hardouin, F.; Achard, M. F.; Jin, J.-I.; Shin, J.-W.; Yun, Y.-K. *J. Phys. France II* **1994**, *4*, 627. (b) Hardouin, F.; Achard, M. F.; Jin, J. I.; Shin, J.-W.; Yun, Y.-K. *J. Phys. France II* **1995**, *5*, 927. (c) Hardouin, F.; Achard, M. F.; Jin, J.-I.; Shin, J.-W.; Yun, Y.-K.; Chung, S. J. *Eur. Phys. J*. **1998**, *B1*, 47. (d) Cha, S.-W.; Jin, J.-I.; Laguerre, M.; Ahard, M. F.; Hardouin, F. *Liq. Cryst.* **1999**, *26*, 1325.
(25) Cha, S.-W.; Jin, J.-I.; Laguerre, M.; Ahard, M. F.; Hardouin, F. *Liq. Cryst.* **2002**, *29*, 755.
(26) (a) Shankar Rao, D. S.; Krishna Prasad, S.; Raja, V. N.; Yelamaggad, C. V.; Anitha Nagamani, S. *Phy. Rev. Lett*. **2001**, *87*, 085504. (b) Yelamaggad, C. V.; Mathews, M.; Fujita, T.; Iyi, N. *Liq. Cryst*. **2003**, *30*, 1079. (c) Yelamaggad, C. V.; Srikrishna, A.; Shankar Rao, D. S.; Krishna Prasad, S. *Liq. Cryst.* **1999**, *26*, 1547. (d) Yelamaggad, C. V.; Anitha Nagamani, S.; Hiremath, U. S.; Nair, G. G. *Liq. Cryst.* **2001**, *28*, 1009. (e) Yelamaggad, C. V.; Mathews, M.; Fujita, T.; Iyi, N. *Liq. Cryst.* **2003**, *30*, 125.

Scheme 1. Synthesis of Unsymmetrical Dimers

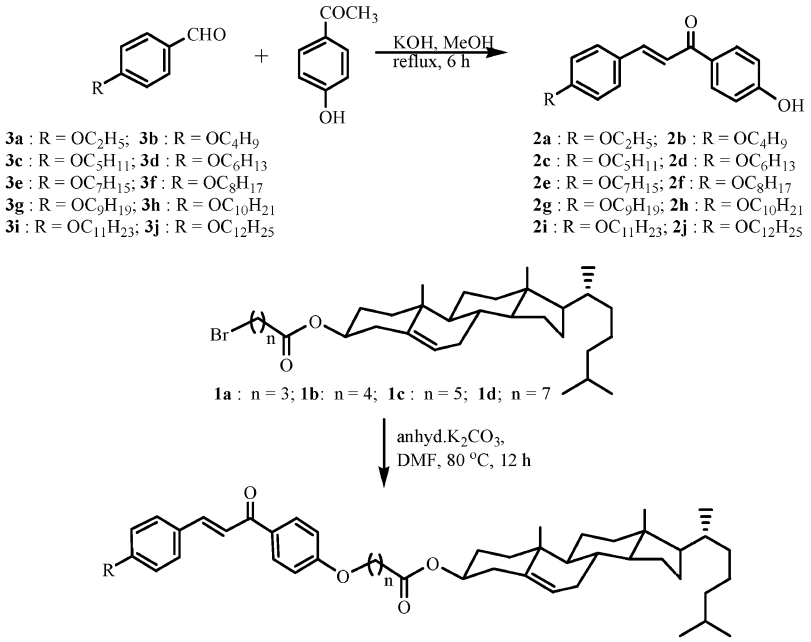

3a : R = OC_2H_5; **3b** : R = OC_4H_9
3c : R = OC_5H_{11}; **3d** : R = OC_6H_{13}
3e : R = OC_7H_{15}; **3f** : R = OC_8H_{17}
3g : R = OC_9H_{19}; **3h** : R = $OC_{10}H_{21}$
3i : R = $OC_{11}H_{23}$; **3j** : R = $OC_{12}H_{25}$

2a : R = OC_2H_5; **2b** : R = OC_4H_9
2c : R = OC_5H_{11}; **2d** : R = OC_6H_{13}
2e : R = OC_7H_{15}; **2f** : R = OC_8H_{17}
2g : R = OC_9H_{19}; **2h** : R = $OC_{10}H_{21}$
2i : R = $OC_{11}H_{23}$; **2j** : R = $OC_{12}H_{25}$

1a : n = 3; **1b**: n = 4; **1c** : n = 5; **1d**; n = 7

Series I : **DC-3,m**

DC-3,2 : n = 3; R = OC_2H_5 (83 %)
DC-3,4 : n = 3; R = OC_4H_9 (84 %)
DC-3,5 : n = 3; R = OC_5H_{11}(85 %)
DC-3,6 : n = 3; R = OC_6H_{13} (86 %)
DC-3,7 : n = 3; R = OC_7H_{15} (84 %)
DC-3,8 : n = 3; R = OC_8H_{17} (85 %)
DC-3,9 : n = 3; R = OC_9H_{19} (86 %)
DC-3,10 : n = 3; R = $OC_{10}H_{21}$ (84 %)
DC-3,11 : n = 3; R = $OC_{11}H_{23}$ (87 %)
DC-3,12 : n = 3; R = $OC_{12}H_{25}$ (85 %)

Series II : **DC-4,m**

DC-4,2 : n = 4; R = OC_2H_5 (87 %)
DC-4,4 : n = 4; R = OC_4H_9 (83 %)
DC-4,5 : n = 4; R = OC_5H_{11}(85 %)
DC-4,6 : n = 4; R = OC_6H_{13} (84 %)
DC-4,7 : n = 4; R = OC_7H_{15} (83 %)
DC-4,8 : n = 4; R = OC_8H_{17} (85 %)
DC-4,9 : n = 4; R = OC_9H_{19} (86 %)
DC-4,10 : n =4; R = $OC_{10}H_{21}$ (87 %)
DC-4,11 : n =4; R = $OC_{11}H_{23}$ (84 %)
DC-4,12 : n = 4; R = $OC_{12}H_{25}$ (86 %)

Series III : **DC-5,m**

DC-5,2 : n = 5; R = OC_2H_5 (86 %)
DC-5,4 : n = 5; R = OC_4H_9 (84 %)
DC-5,5 : n = 5; R = OC_5H_{11}(85 %)
DC-5,6 : n = 5; R = OC_6H_{13} (83 %)
DC-5,7 : n = 5; R = OC_7H_{15} (84 %)
DC-5,8 : n = 5; R = OC_8H_{17} (86 %)
DC-5,9 : n = 5; R = OC_9H_{19} (85 %)
DC-5,10 : n = 5; R = $OC_{10}H_{21}$ (85 %)
DC-5,11 : n = 5; R = $OC_{11}H_{23}$ (87 %)
DC-5,12 : n = 5; R = $OC_{12}H_{25}$ (85 %)

Series IV : **DC-7,m**

DC-7,2 : n = 7; R = OC_2H_5 (84 %)
DC-7,4 : n = 7; R = OC_4H_9 (84 %)
DC-7,5 : n = 7; R = OC_5H_{11}(85 %)
DC-7,6 : n = 7; R = OC_6H_{13} (87 %)
DC-7,7 : n = 7; R = OC_7H_{15} (86 %)
DC-7,8 : n = 7; R = OC_8H_{17} (85 %)
DC-7,9 : n = 7; R = OC_9H_{19} (83 %)
DC-7,10 : n =7; R = $OC_{10}H_{21}$ (84 %)
DC-7,11 : n = 7; R = $OC_{11}H_{23}$ (87 %)
DC-7,12 : n = 7; R = $OC_{12}H_{25}$ (85 %)

Table 1. Photophysical Properties of Representative Dimers

		emission	
compd	absorption	λ_{ex} 294 nm	λ_{ex} 310 nm
DC-4,10	235.2, 337	344, 443.5, 484	439, 484.5
DC-4,11	243.8, 337.4	343, 423, 484.5	424.5, 485
DC-4,12	233.8, 323.6	342.5, 246, 485	423.5, 484

incommensurate phase than for the appearance of other frustrated phases viz. the BP and TGB phases. [24c,d] Interestingly, anomalies of periodicity occurring in the TGB structures have also been reported.[25] In an effort to stabilize similar mesophases, we have been exploring the possibility of attaching different types of chiral or achiral aromatic mesogenic cores to the cholesteryl ester unit through odd−even parity spacer.[26] Remarkably, it has been found that the dimers having diphenylacetylene,[26a,b] Schiff's base,[26c] and biphenyl [26d,e] mesogenic cores exhibit frustrated phases viz, BP, TGB, and TGBC* phases in polymorphic sequences including reentrant TGB phase. Because no general conclusion can be inferred on which molecular fragments such as aromatic core and spacer make the resulting dimeric system strongly chiral so as to form frustrated phases, it appears that further studies involving molecular engineering and synthesis are essential.

Thus, in the development of new materials characterized by strong chirality, it occurred to us that a bent-core could be covalently linked to the cholesterol entity. In this context, a 4,4′-disubstituted (*E*)-chalcone core in which two phenyl rings are connected thorough an α,β-unsaturated ketone group (odd number of atoms) giving rise to a bent structure to the core appear to be an appropriate aromatic entity.[27] In addition, chalcones are known for their potential as fluorescence materials, a feature attractive from both biological and material sciences points of view.[28] The expectation of the enhancement of chirality in such systems was substantiated by our recent observation,[29] in which the chalcone unit connected to cholesterol unit through an odd-parity spacer stabilized the frustrated phases over a wide thermal range.[29] This inspired us to synthesize dimeric analogues of these reported systems in which the length and parity of spacer as well as length of terminal tails were varied. In particular, we synthesized and characterized the thermal behavior of novel fluorescent unsymmetrical liquid crystal dimers in which the cholesterol is covalently connected to (*E*)-1-(4-*n*-alkoxyphenyl)-3-(4-hydroxyphenyl) prop-2-en-1-one (chalcone) core through an alkylene spacer. To understand the relation between the molecular structure−liquid crystal properties, the length and parity of the central spacer as well as the length of the terminal tail have been varied. The mnemonic employed for these series of compounds is **DC-*n,m***, where DC represents dimeric chalcone, *n* indicates

(27) Chudgar, N. K.; Shah, S. N. *Liq. Cryst.* **1989**, *4*, 661.
(28) (a) Valeur, B. In *Molecular Fluorescence: Principle and Applications*; Valeur, B., Ed.; Wiley-VCH: Weinheim, Germany, 2002. (b) Chandran, S. S.; Dickson, K. A.; Raines, R. T. *J. Am. Chem. Soc.* **2005**, *127*, 1652.
(29) Yelamaggad, C. V.; Achalkumar, A. S.; Bonde, N. L.; Prajapati, A. K. *Chem. Mater*. **2006**, *18*, 1076.

Table 2. Transition Temperatures (°C)[a] and Enthalpies (J/g) of 4-*n*-alkoxy-4′-(cholesteryloxycarbonyl-1-propyloxy)chalcones (Series I; DC-3,m)[b]

	phase sequence	
dimer	heating	cooling
DC-3,2	Cr_1 155.4 (17.3) Cr_2 171.9 (72.7)I	I 168.8[c] BP 167.6[c] N* 144.1(35.9) Cr
DC-3,4	Cr_1 153.5 (18.5) Cr_2 162.6 (50.3) I	I 156.6 (0.5) BP 154.1 (0.2) N* 146.1 (35.9) Cr
DC-3,5	Cr_1 158.2 (56) I	I 153.7 (1.2) BP 152.3[c] N* 138.1(37) Cr
DC-3,6	Cr_1 131.4 (7.1) Cr_2 141.2 (64.3) I	I 140[c] BP 138.7[c] N* 125 (0.8)[d] SmA 100 (17.8) Cr
DC-3,7	Cr_1 153.8 (50.7) I	I 151.9 (0.5) BP 150.7 (0.1) N* 144.7 (0.1) TGB 143.7 (0.3) SmA 133.4 (34.7) Cr
DC-3,8	Cr_1 116.9 (17.5) Cr_2 148.8 (51.4) SmA 152.8 (1.5) I	I 148 (1.5) BP 146.7[c] N* 143.2 (0.5)[d] SmA 126.8 (33.9) Cr
DC-3,9	Cr_1 117.2 (14.1) Cr_2 145.8 (34.2) SmA 150.5 (1.9) N* 152.1 (2.2) I	I 151.2 (2.1)[e] N* 149.4 (1.9)[d] SmA 125 (28.1)Cr
DC-3,10	Cr_1 135.4 (70.4) Cr_2 140.8 (7.5) SmA 150.8 (7.5) I	I 149.3 (6.8)[f] SmA 116.6 (24.9) Cr
DC-3,11	Cr 138.1 (72.2) SmA 150.5 (8.2) I	I 146.5 (6) SmA 101.4 (15.1) Cr
DC-3,12	Cr 136.8 (69) SmA 151.8 (8.4) I	I 146.8 (6.1) SmA 97.1 (11.9) Cr

[a] Peak temperatures in the DSC thermograms obtained during the first heating and cooling cycles at 5 °C/min. [b] The enthalpy values are enclosed in brackets. Acronyms used (applicable wherever used): *I* = isotropic liquid state; BP = blue phase; N* = chiral nematic phase; TGB = twist grain boundary phase (with either SmA or SmC blocks); SmA = smectic A phase; SmC* = chiral smectic C phase; Cr = crystal. [c] The phase transition was observed under POM but too weak to be seen in the DSC scans. [d] The N*−SmA transition passes through a transient TGB phase. [e] The I−N* transition passes through a transient BP. [f] The I−SmA transition passes through transient BP and N* phases.

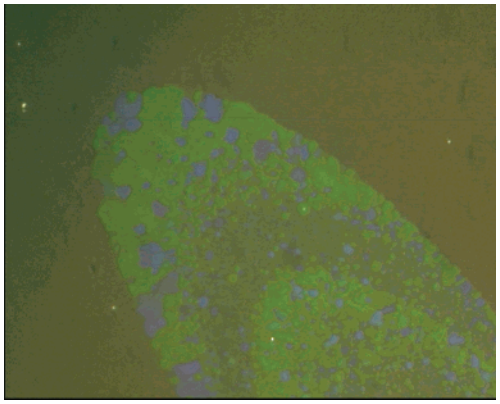

Figure 1. Microphotograph of the platelet textural pattern of the BP observed for the dimer **DC-3,4** at 156 °C during slow cooling (0.2 °C/min) from the isotropic phase.

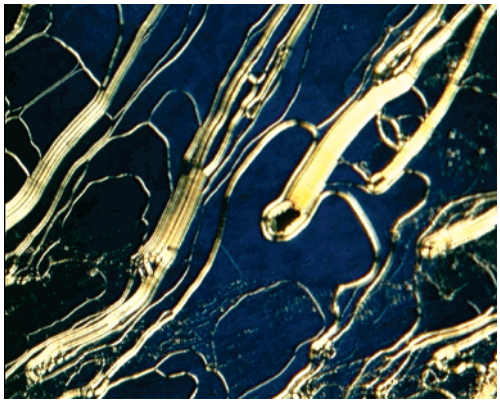

Figure 2. Microphotograph of the oily streak texture of the N* phase obtained for the dimer **DC-3,4** at 148 °C.

the number of methylene units in the central spacer, and *m* represents the number of carbon atoms in the terminal alkoxy chain.

Synthesis and Molecular Structural Characterization

The synthetic steps employed to unsymmetrical dimers and their precursors have been depicted in the Scheme 1. The key intermediates, chalcones (α,*β*-unsaturated arylketones) **2a**−**j**, were obtained in almost quantitative yield by the Claisen−Schmidt reaction, in which 4-hydroxyacetophenone was condensed with various 4-(*n*-alkoxy)benzaldehydes (**3a**−**j**) in the presence of a strong base. On the other hand, cholesteryl *ω*-bromoalkanoates **1a**−**d** were prepared by coupling commercially available optically pure cholesterol with alkanoyl chlorides using pyridine as a mild base and THF as solvent. Finally, the target unsymmetrical dimers **DC-*n,m*** were obtained in a reasonable yield (83−87%) when chalcones were coupled with cholesteryl *ω*-bromoalkanoates **1a**−**d** by employing Williamson's ether synthesis protocol. The unsymmetrical dimers were characterized systematically by IR, UV−vis, NMR (^{1}H and ^{13}C), and mass spectrometry, as well as by elemental analysis (see the Supporting Information for details). Although the spectral data of all the chalcones **2a**−**j** were found to be consistent with their molecular structure, in some cases, the melting points determined with the help of a polarizing microscope and differential scanning calorimeter (DSC) were found to be slightly different from the reported[27] value as indicated in the Supporting Information.

The optical activity (specific rotation [α]) of all the chiral dimers were obtained by optical rotatory dispersion (ORD) data using a Jasco DIP-370 digital polarimeter from their solutions (c = 1 in CH_2Cl_2). All the dimers were found to be levorotatory with the specific rotation values in the range of −11 to −26 (see the Supporting Information). As expected, the spectroscopic spectra of all the unsymmetrical dimers almost look alike, with few negligible exceptions. The UV−vis (absorbance) spectra of the dimers in solution (CH_2Cl_2) display two absorption maxima, in the region 286−295 (ϵ = 0.8−2.3 × 10^6 mol^{-1} dm^3 cm^{-1}) and 338−342 (ϵ = 1−2.8 × 10^6 mol^{-1} dm^3 cm^{-1}), whereas the UV−vis spectra of the representative dimers in the solid film state showed absorption maxima in the regions 233−235 and 323−337 nm. For the same representative samples, the fluorescence (emission) spectra in their solid state at room temperature (30 °C) were recorded for the two different excitation wavelengths viz., 294 and 310 nm (see the Supporting Information). For the excitation wavelengths 294 nm, these compounds exhibit three emission bands in the

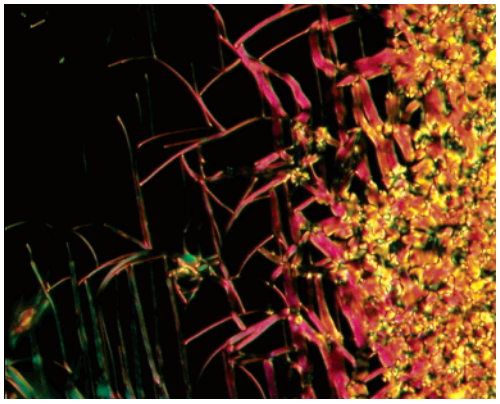

Figure 3. Microphotograph of the texture obtained at the N*−SmA transition for the dimer **DC-3,8** at about 143.2 °C. Notice that the textures corresponding to the SmA (dark field of view), TGB (filaments), and N* (extreme right portion, nonspecific) coexisting.

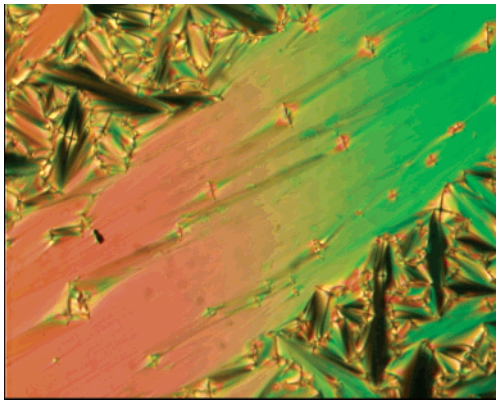

Figure 4. Microphotograph of the focal-conic texture of the SmA phase observed for the dimer **DC-3,12** at 124 °C.

ranges of 342−344, 423−443.5, and 484−485 nm with some negligible shoulders (Table 1). When the same solids were excited at 310 nm, two emission maxima in the regions of 423.5−439 and 484−485 were observed. It is apparent that a small hypsochromic effect (blue shift) occurs with the increase in the chain length of the terminal tail (see the Supporting Information). These spectroscopic data ascertain the fluorescence property of these unsymmetrical dimers.[30a] As mentioned earlier, several different series of cholesterol-based unsymmetrical dimers have been described in the literature, but very few dimers containing a fluorescent entity have been reported hitherto.[30b]

Mesomorphic Behavior

Four series of unsymmetrical dimers are formed as a consequence of variations in the length and parity of the central flexible alkylene spacer (*n*) as well as the lengths of the terminal alkyl tails (*m*). In series I (**DC-3,m**), II (**DC-4,m**), III (**DC-5,m**) and IV(**DC-7,m**), two mesogenic segments are separated by a trimethylene ($n = 3$, 4-oxybutanoyl, even spacer), tetramethylene ($n = 4$, 5-oxypentanoyl, odd spacer), pentamethylene ($n = 5$, 6-oxyhexanoyl, even spacer), and heptamethylene ($n = 7$, 8-oxyoctanoyl, even spacer)

(30) (a) Lakowicz, J. R. In *Principles of Fluorescence Spectroscopy*, 2nd ed.; Lakowicz, J. R., Ed.; Plenum Publishing: New York, 1999. (b) Abraham, S.; Mallia,V. A.; Ratheesh, K. V.; Tamaoki, N.; and Das, S. *J. Am. Chem. Soc.* **2006**, *128*, 7692.

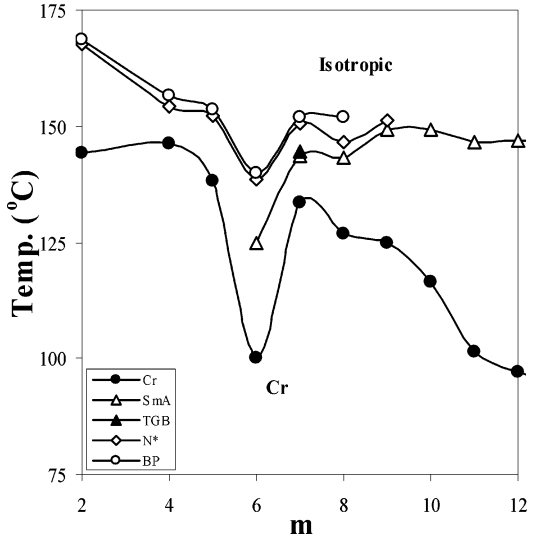

Figure 5. Plot of transition temperatures as a function of alkoxy tail length (*m*) for the compounds of series I (**DC-3, m**).

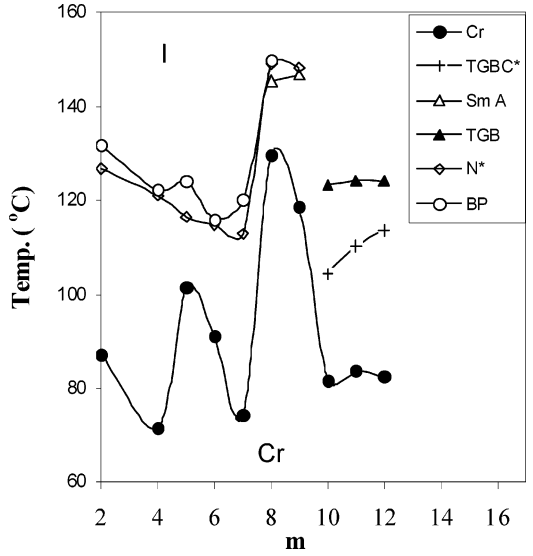

Figure 6. Plot of transition temperatures as a function of alkoxy tail length (*m*) for the compounds of series II (**DC-4, m**).

central spacer. In each series, the chalcone entity is substituted with ethoxy ($m = 2$), *n*-butyloxy to *n*-dodecyloxy ($m = 4-12$) tails that gave rise to 10 homologues. Liquid crystal properties of these four series of compounds were investigated mainly with the help of polarizing optical microscope (POM) and differential scanning calorimeter (DSC). As representative cases, DSC thermograms obtained during the first heating and cooling cycles at a rate of 5 °C/min for the dimers **DC-4,10**, **DC-4,11**, and **DC-4,12** have been shown (see the Supporting Information). The phase sequences, transition temperatures, and enthalpies of dimers of series I, **DC-3,m** are presented in Table 2.

The lower homologues **DC-3,2**, **DC-3,4**, and **DC-3,5** exhibit monotropic blue phase (BP) and chiral nematic (N*) phases that were ascertained by the observation of characteristic textural pattern. These samples, on slow cooling (0.2 °C/min.) from their isotropic phase, exhibit a uniform blue color of low birefringence before a platelet texture composed of blue and green plates quickly grows with crinkled lines (Figure 1) that upon mechanical shearing yield

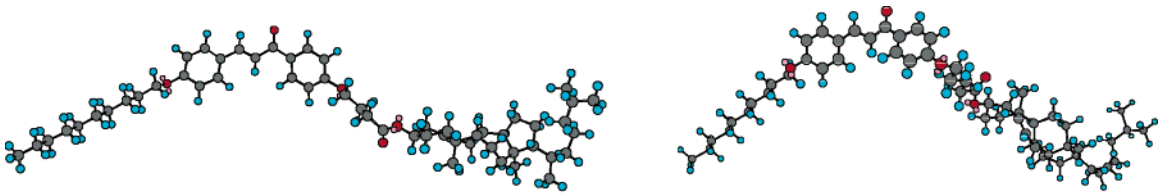

DC-3,10 **DC-4,10**

Figure 7. Energy-minimized (MM2 models derived from CS ChemDraw Ultra 5.0 software) structures of dimers **DC-3,10** and **DC-4,10**. Notice that mesogenic groups of the dimer **DC-4,10** possessing an odd-parity spacer is more twisted than the corresponding even dimer **DC-3,10**.

Table 3. Transition Temperatures (°C)[a] and Enthalpies (J/g) of 4-*n*-alkoxy-4′-(cholesteryloxycarbonyl-1-butyloxy)chalcones (Series II; DC-4,m)

	phase sequence	
dimer	heating	cooling
DC-4,2	Cr_1 111.4 (38.3) Cr_2 125.3 (48.9) N* 128.1 (0.4) BP 132.4 (1.6) I	I 131.6 (1.5) BP 126.8 (0.4) N* 87(42.6) Cr
DC-4,4	Cr_1 110.0 (47) Cr_2 117.5 (34.4) N* 125.5 (1.5) I	I 122.3 (1.1) BP 121.0 (0.2) N* 71.6 (17.8) Cr
DC-4,5	Cr_1 126.1 (60.3) I	I 124.1 (1.4) BP 116.5[b] N* 101.5(43.7) Cr
DC-4,6	Cr_1 132.2 (48.2) I	I 116 (1.2) BP 114.8 (0.4) N* 91 (35.5) Cr
DC-4,7	Cr_1 132.5 (62) I	I 120.0 (2) BP 112.9 (0.3) N* 74.4 (27.2) Cr
DC-4,8	Cr_1 116.2 (12.8) Cr_2 149.1 (42.9) N* 152.0 (2.2) I	I 149.8 (2.0) BP 149.0[b] N* 145.4 (1.0)[c] SmA 129.6 (29.9) Cr
DC-4,9	Cr_1 113.3 (15.4) Cr_2 144.2 (41.3) SmA 148.9 (2.3) N* 150.5 (1.7) I	I 148.3 (1.6)[d] N* 146.7 (2.2)[c] SmA 118.6 (26.1) Cr
DC-4,10	Cr_1 118.9 (46.0) TGB 124.4 (6.2) I	I 123.3 (6.2) TGB 104.4[b] TGBC* 81.6 (20.2) Cr
DC-4,11	Cr 114.2 (41.1) TGB 125.4 (7.8) I	I 124.2 (7.7) TGB 110.2[b] TGBC* 83.6 (23.9) Cr
DC-4,12	Cr_1 114.2 (29) Cr_2 116.3 (8.6) TGB 125.9 (7) I	I 124.1 (7) TGB 113.6[b] TGBC* 82.5 (16.3) Cr

[a] Peak temperatures in the DSC thermograms obtained during the first heating and cooling cycles at 5 °C/min. [b] The phase transition was observed under POM but was too weak to be seen in the DSC scans. [c] The N*−SmA transition passes through a transient TGB phase, which can have either SmA or SmC blocks. [d] The I−N* transition passes through a transient BP.

a Grandjean plane texture indicating the presence of the blue phase I (BPI). On further cooling, red plates also grow in addition and concomitantly, a nonspecific birefringent texture appears on top of the platelet pattern, which on shearing gives rise to the oily streaks characteristic of the Grandjean planar texture of the N* phase as shown in Figure 2.

The transition to blue phase could be detected in DSC thermograms for the compounds **DC-3,4** and **DC-3,5**. The thermal range of blue phase in these compounds is 1−2 °C. The intermediate homologues of the series **DC-3,6**, **DC-3,7**, **DC-3,8**, and **DC-3,9** exhibit a polymorphic sequence. These dimers, when placed on clean glass slides and cooled at a rate of 0.2 °C /min from their isotropic phase, exhibit a foggy pattern without any structure, which when sheared displayed the characteristic Grandjean planar texture, suggesting that these compounds exhibit blue phase III (BPIII). As we shall see later, similar observations were made for all the dimers, except for the dimers **DC-3,2**, **DC-3,4**, and **DC-3,5**. On cooling, the unperturbed foggy pattern shows a pseudo focal-conic fan texture (which upon shearing furnishes an oily streak texture), indicating the occurrence of the N* phase. On further cooling, the N* phase transforms into the SmA phase through a transient TGB phase that was ascertained on the basis of the observation of pseudoisotropic (homeotropic) pattern occurring via filament structure. It may be pointed out here that the TGB phase may have either SmA or SmC slabs. The occurrence of SmA mesophase was further evidenced on the basis of the microscopic observation of characteristic focal-conic texture in slides treated for planar orientation and a dark field of view in slides treated for homeotropic orientation. The TGB phase showed the filament or planar textural pattern, respectively, when heated from a homeotropic or planar (with focal-conic pattern) SmA phase. In these compounds, because of a very narrow thermal range of TGB phase, N* and SmA phases coexisted along with TGB, which was evident from the fact that the textures corresponding to these three mesophases appear simultaneously over a narrow range of temperature (Figure 3). The higher homologue **DC-3,10** comprising *n*-decyloxy tail exhibits the SmA through a short existence of both N* and BP phases. The absence of the TGB phase, in this particular case, may be due to the intercalated nature of the SmA phase, as it is possible that such a structure of the SmA phase inhibit the layers from twisting into a helix. The next-higher homologues **DC-3,11** and **DC-3,12** display an enantiotropic SmA phase over only a relatively wide thermal range. Figure 4 shows the characteristic fan-shaped texture observed for the compound **DC-3,12**.

The plot of temperature vs length of the terminal tail (*m*) (Figure 5) shows that increasing *m* decreases the mesophase to the isotropic phase-transition temperature and supports the formation of layered structure. The stabilization of the smectic mesophase for the dimers having a long chain can obviously be attributed to the increase of the side-on and weakening of the terminal intermolecular interactions, which is in agreement with the general observation made for cholesterol-based monomeric materials.[20a]

It can be noticed that dimers having a tetramethylene (5-oxypentanoyl) central spacer exhibit relatively low clearing temperatures when compared with other series of compounds, a feature that can be explained as follows. In these dimers, the cholesterol moiety and the chalcone core are linked to the alkylene spacer via a carbonyl group and an ether linkage, respectively. In these and similar type of compounds (dimers), the conventional way of accounting for the parity of the spacer is to consider only the number of carbon atoms of methylene units (as in our presentation). For example, dimers of series **DC-4,m** series are considered to be even-

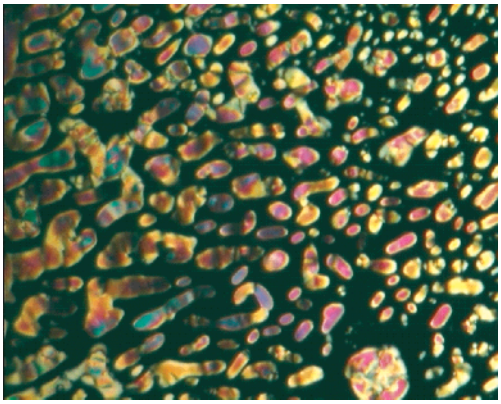

Figure 8. Microphotograph of the TGB phase separating from the isotropic liquid observed for the dimer **DC-4,12** at 123.8 °C. Notice the coalescence of the TGB droplets to furnish both planar (see left top corner) and blur fanlike textures.

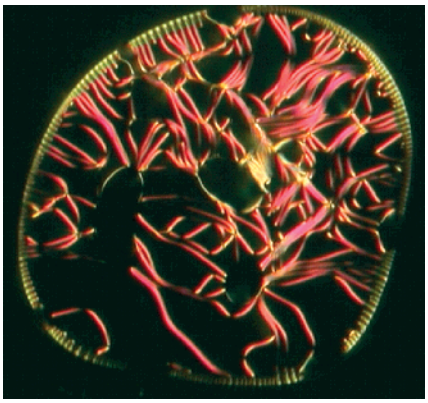

Figure 9. Microphotograph of the filament textural pattern of the TGB phase grown around the air packets for the dimer **DC-4,12** at 120 °C.

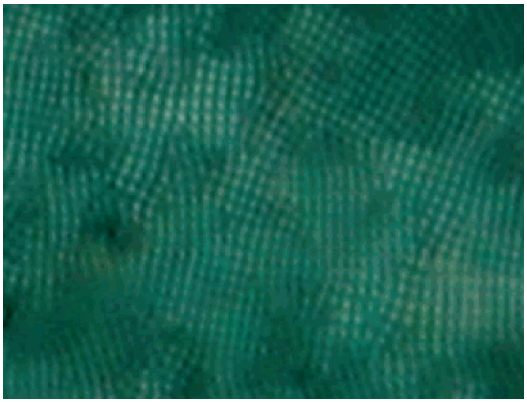

Figure 10. Microphotograph displaying the square grid pattern of the TGBC* phase of a homogeneously aligned sample **DC-4,11** at 110 °C.

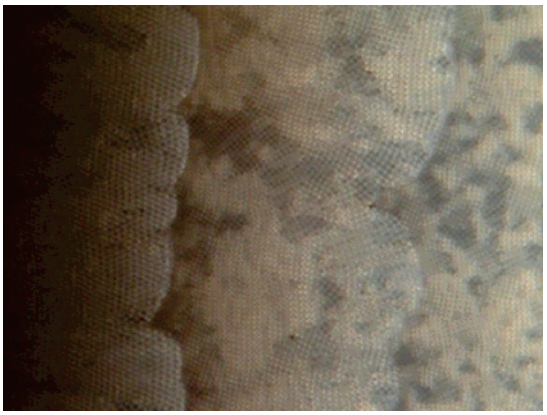

Figure 11. Microphotograph of the TGBC* phase observed at 108 °C for the dimer **DC-4,11** while cooling from the TGB phase. Notice that Grandjean Cano lines (the two distorted striations running from top to the bottom of the picture) superposed on the square pattern.

members because four methylene units separate the two rigid cores, whereas if the carbon atom of carbonyl group is also taken as a part of the central spacer, then they would become odd-members. Table 3 presents the phase sequences, transition temperatures, and enthalpies of dimers of series II (**DC-4,m**). Figure 7 shows the molecular shapes of the dimers **DC-3,10** and **DC-4,10** in the respective all-trans conformation (energy-minimized models derived from CS ChemDraw Ultra 5.0), from which it can be noticed that the mesogenic groups of the dimer **DC-4,10** with an odd-parity spacer are more twisted than those of the corresponding even dimer **DC-3,10**.

The lower homologues of the series, **DC-4,2** and **DC-4,4** to **DC-4,7**, display the BP and N* phases. Remarkably, **DC-4,2**, **DC-4,5**, and **DC-4,7** stabilize blue phase over a relatively wide temperature range (4−7 °C). While cooling from their isotropic phase, the intermediate homologues, **DC-4,8** and **DC-4,9**, show BP, N*, TGB, and SmA phases, as evidenced in a manner explained earlier. However, the higher homologues, **DC-4,10**, **DC-4,11**, and **DC-4,12**, were found to exhibit an interesting dimorphic sequence involving a transition between two frustrated phases. The crystalline compounds **DC-4,10**, **DC-4,11**, and **DC-4,12** placed on clean glass slides were heated to isotropic state and, when cooled slowly (at a rate of 0.2 °C /min,), a transition to the twist grain boundary phase (TGB) occurs at 123.3, 124.2, and 124.1 °C, respectively, with a textural pattern described below.[17a] The usage of an ordinary slide made it possible to visualize the optical textural patterns arising because of both homogeneous (planar) and homeotropic alignment of the molecules. Initially, the mesophase grows as droplets, which upon slight cooling begin to coalesce to a pattern as shown in Figure 8 for the dimer **DC-4,12** as a representative case. On further cooling, the Grandjean planar (with a dull gray background) as well as a blurred pseudo-focal conic fan textures were observed in different regions of the slide. More importantly, at the edges of slide and around the air packets, filaments were found to occur predominantly (see Figure 9), which is conclusive evidence for the presence of TGB phase.

When thin samples were examined on slides treated for planar condition (orienting the molecular long axis with the smectic layer planes perpendicular to the glass plates), Grandjean planar texture with a dull gray colored background was observed. With homeotropic anchoring conditions in which the helix axis lies in the plane of the bounding glass plates, a beautiful filament texture is seen that in the majority of the area coalesces to a sort of fanlike texture as the temperature is lowered in the TGB phase. On the other hand, preparation of the sample in a wedge cell treated for planar geometry and continuous variation in the thickness of the cell from one end to other results in an array of equidistant Grandjean−Cano (GC) dislocation lines (striations running

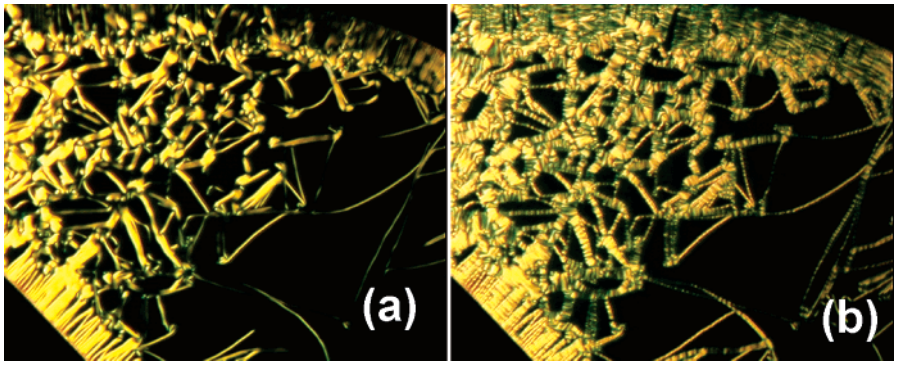

Figure 12. Microphotograph of the transition from (a) filaments of TGB at 113.7 °C to (b) undulated filaments of TGBC* phase observed for the dimer **DC-4,12** at 100 °C in the same sample area.

from the top to bottom of the pattern). All these optical observations unambiguously ascertain the occurrence of the I-TGB phase transition that makes the **DC-4,m** compounds the third set of novel mesogens exhibiting this sequence.[31,32] On cooling further, the TGB phase transforms into another TGB mesophase[33−35] featuring smectic C* blocks (TGBC*) at about 104.4 , 110.2, and 113.6 °C, respectively, for the dimers **DC-4,10**, **DC-4,11**, and **DC-4,12** (see later sections for details). These dimers thus stabilize the TGB structure over a wide thermal range viz., 10−18 °C, which is remarkable in light of the fact that in all known single-component systems, the temperature range of the TGB phase rarely exceeds a few degrees Celsius.[3,31] However, in a few mixtures as well as in some other systems, the thermal rage of the TGB phase has been remarkably wide (40 °C).[3,32]

The structure of the TGBC* phase is obviously more complicated than those of TGBA and TGBC phases.[3,34] According to Galerne,[34] in addition to the tilt of the molecules with respect to the smectic layer normal as in TGBC phase, there is a precision of the SmC director, resulting in a second helix orthogonal to the TGB helix axis; consequently, each smectic block has a smectic C* structure. A direct consequence of this is the appearance of the square grid pattern. Experimentally, it has been observed that the TGBC* phase indeed exhibits a square grid pattern superimposed on the planar texture.[3]

These dimers, when investigated in slides treated for homogeneous alignment and cooled from the planar texture of the high-temperature TGB phase, showed a transformation to a well-aligned square grid pattern (Figure 10) at the temperatures 104.4, 110.2, and 113.6 °C, respectively, for the dimers **DC-4,10**, **DC-4,11**, and **DC-4,12**. To ascertain that the observed square grid pattern is not due to some instabilities in the SmC* phase, these dimers were studied in wedge-shaped cells. Whilte the high-temperature TGB phase exhibiting GC is cooled, a square grid pattern appears over these dislocation lines and fills the entire field of view at the transition to TGBC* phase (Figure 11).

The GC lines indicate the presence of TGB helical superstructure (twist axis perpendicular to the substrate), whereas the square grid patterns originate from the two-dimensional director modulation in the plane of the substrate, presumably due to the SmC* pitch. The simultaneous existence of both features is supposed to be the proof of the existence of the TGBC* phase. On the other hand, when examined on slides treated for homeotropic anchoring conditions and cooled from the filament texture of TGB phase, transition to TGBC* phase is signified by the filaments becoming undulated. A representative case of the change from the straight filament pattern to undulated filament textural pattern observed for the dimer **DC-4,12** is shown in Figure 12.

In light of the fact that the TGBC* phase is a highly frustrated phase, its occurrence over the thermal range of 22−30 °C in these dimers is noteworthy. It is apparent that the thermal range of high-temperature TGB phase gets reduced with the enhancement in the temperature range of TGBC* phase as the length of terminal tail is increased. Thus, unsymmetrical dimers **DC-4,10**, **DC-4,11**, and **DC-4,12** exhibit a new liquid crystal phase sequence viz., I-TGB-TGBC*. The TGB phase occurs for a relatively wide thermal range, i.e., 10−18 °C, which is remarkable considering the general observation that such frustrated fluids do not exist for more than 1 °C in single-component systems. Another interesting and noticeable aspect is that optically active molecular architectures exhibiting a direct transition from isotropic liquid phase to twist grain boundary phase are rarely reported.[17a,31,33]

Phase-transition temperatures, phase sequences, and transition temperatures of dimers belonging to series III (**DC-5,m**) and IV (**DC-7,m**), respectively, are summarized in Table 4 and 5 and graphically shown in Figures 13 and 14. As can be seen from Table 4, the first member **DC-5,2** of series III is non-mesomorphic, whereas the lower homologues **DC-5,4** to **DC-5,9** stabilize monotropic N* and BP phases over a short thermal range.

The dimer **DC-5,10** having *n*-decyloxy tail displays the BP, N*, TGB, and SmA phases, whereas the next homologue **DC-5,11** exhibits similar behavior except that the TGB phase

(31) An interesting TGB phase characterized by both columnar and smectic ordering has been reported to be stable over a temperature range of 20 °C: Ribeiro, A. C.; Dreyer, A.; Oswald, L.; Nicoud, J. F.; Soldera, A.; Guillon, D.; Galerne, Y. *J. Phys. France II* **1994**, *4*, 407.
(32) (a) Nguyen, H. T.; Destrade, C.; Parneix, J. P.; Pochat, P.; Isaert, N.; Girold, C. *Ferroelectrics* **1993**, *147*, 181. (b) Terris, B. D.; Twieg, R. J.; Nguyen, G.; Sigaud, G.; Nguyen, H. T. *Europhys. Lett.* **1992**, *19*, 85.
(33) Kuczynski, W.; Stegeyer, H. *Mol. Cryst. Liq. Cryst.* **1995**, *260*, 377.
(34) Galerne, Y. *Eur. Phys. J. E* **2000**, *3*, 355.
(35) Pramod, P. A.; Pratiba, R.; Madhusudana, N. V. *Curr. Sci.* **1997**, *73*, 761.

Table 4. Transition Temperatures (°C)[a] and Enthalpies (J/g) of 4-*n*-alkoxy-4′-(cholesteryloxycarbonyl-1-propyloxy)chalcones (Series III; DC-5,m)

	phase sequence	
dimer	heating	cooling
DC-5,2	Cr_1 189.9 (90.4) I	I 166.0 (82.8) Cr
DC-5,4	Cr_1 125.2 (20.9) Cr_2 156.1 (55.4) I	I 147.7 (1.3) BP 146.4[b] N* 144.5 (11) Cr
DC-5,5	Cr_1 112.7 (5.4) Cr_2 150.7 (48.4) I	I 142.9 (1.2) BP141.5[b] N* 137.4 (34.5) Cr
DC-5,6	Cr_1 121.1 (9.2) Cr_2 148.3 (50.2) I	I 137.3 (0.3) BP 135.9 (0.4) N* 130.9 (31.3) Cr
DC-5,7	Cr_1 120.5 (5.6) Cr_2 147 (47.3) I	I 139.8[b] BP138.5[b] N* 135.2(34.4) Cr
DC-5,8	Cr_1 113.3 (20.3) Cr_2 144.5 (47.5) I	I 138.7 (1.8) BP 136.8[b] N* 134.5 (39.5) Cr
DC-5,9	Cr_1 111.2 (10.1) Cr_2 141.5 (47.8) I	I 136.8 (2.3) BP 134.9[b] N* 132.5 (39.2) Cr
DC-5,10	Cr_1 106.3 (9) Cr_2 138 (40.2)	I 135.7[b] BP 133.4[b] N* 132.9 (1.3)[c] SmA 125.5 (22.4) Cr
DC-5,11	Cr_1 107.2 (10.4) Cr_2 136.4 (44.2) I	I 135.2 (0.7) N* 134.3 (1.4) SmA 123.5 (28.1) Cr
DC-5,12	Cr_1 119.5 (6.4) Cr_2 135.1 (16.6) SmA 137.2 (3.7) I	I 136.1 (3.7) SmA 122.6 (13.3) Cr

[a] Peak temperatures in the DSC thermograms obtained during the first heating and cooling cycles at 5 °C/min. [b] The phase transition was observed under polarizing microscope but was too weak to get recognized in DSC. [c] The N*−SmA transition passes through a transient TGB phase.

Table 5. Transition Temperatures (°C)[a] and Enthalpies (J/g) of 4-*n*-alkoxy-4′-(cholesteryloxycarbonyl-1-heptyloxy)chalcones (Series IV; DC-7,m)

	phase sequence	
dimer	heating	cooling
DC-7,2	Cr_1 151(76.6) I	I 140.8[b] BP 136.5(0.9) N*115.4(35.8) Cr
DC-7,4	Cr_1 113.6 (17.6) Cr_2 161.1 (60.5) I	I 147.7 (1.3) N* 135.3 (45.8)Cr
DC-7,5	Cr_1 148.1 (67) I	I 131.2[b] BP 128.2 (1.9) N* 112.6(34) Cr
DC-7,6	Cr_1 127.8(19.8) Cr_2 152.2 (42.1) I	I 130.2[b] BP 128.8[b] N* 124.6 (26.9) Cr
DC-7,7	Cr_1 96.1(25) Cr_2 128.4 (38.4) N* 130.2 (2.1) I	I 129.0 (2.1) BP 125[b] N* 110.4 (31.3) Cr
DC-7,8	Cr 106.8 (28.1) Cr 126.6 (39.8) N* 129.7 (2) I	I 128.8 (2.1) BP 125[b] N* 110.4 (31.3) Cr
DC-7,9	Cr_1 96.3 (27.6) Cr_2 123.7 (37.4)[c] SmA 128.0 (2.3) I	I 126.7 (2.3) BP 122.6[b] N* 113.4[b,c] SmA 102.1 (26.8) Cr
DC-7,10	Cr_1 97 (42.9) Cr_2 119.8 (33.6) SmA 125.5[b,c] N* (7.5) BP 126.1(2.4) I	I 123.4 (2.4) BP 122.8[b] N* 114.8[b,c] SmA 99 (23) Cr
DC-7,11	Cr 70.1 (13.6) Cr 116 (27.7) SmA 117.8 (0.5)[c] N* 121[b] BP 122.5 (2.7) I	I 120.3(2) BP 122[b] N* 119.9[b,c] SmA 90.9 (20.9) Cr
DC-7,12	Cr 115 (26.5) Cr 121 (2) SmA 120.9[b,c] N* 123[b] BP 123.9(2.7) I	I 122.7 (2.7) BP 122[b] N* 119.9[b,c] SmA 90.9 (20.9) Cr

[a] Peak temperatures in the DSC thermograms obtained during the first heating and cooling cycles at 5 °C/min. [b] The phase transition was observed under polarizing microscope but was too weak to get recognized in DSC. [c] The N*−SmA transition passes through a transient TGB phase.

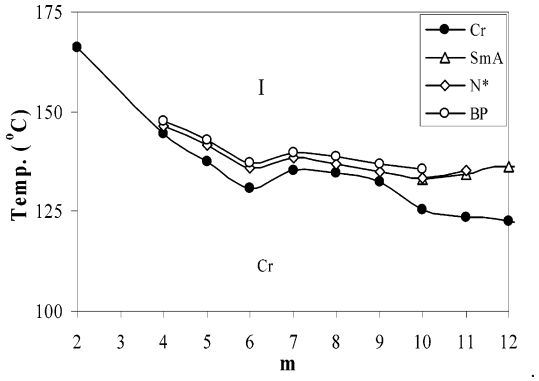

Figure 13. Plot of transition temperatures as a function of alkoxy tail length (*m*) for the compounds of series III (**DC-5, m**).

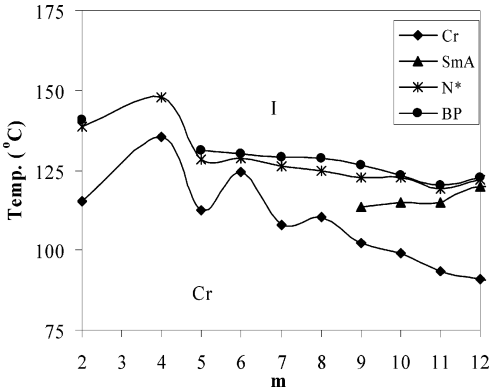

Figure 14. Plot of transition temperatures as a function of alkoxy tail length (*m*) for the compounds of series IV (**DC-7, m**).

gets eliminated. However, the dimer **DC-5,12** displays an enantiotropic SmA phase only, clearly demonstrating the sensitivity of the thermal behavior to the length of the terminal alkoxy tail.

For the series IV (**DC-7,m**), an almost similar relation between liquid crystal behavior and length of terminal tail was found with very few exceptions when compared with other series of compounds. The lower homologues **DC-7,2**, **DC-7,5**, and **DC-7,6** of the series exhibit monotropic BP and N* phases with the surprising exception that **DC-7,4** does not show blue phase. Dimers **DC-7,7** and **DC-7,8** exhibited enantiotropic N* phase. Compounds **DC-7,9** to **DC-7,12** display an identical polymorphic sequence on cooling, suggesting that in these dimers, unlike the compounds of other series with identical chain lengths, the length of the terminal tail has hardly any influence on the thermal behavior. While cooling from their isotropic phase, these dimers exhibit BP, N*, TGB, and SmA phases.

X-ray Studies

To ascertain lamellar ordering of the TGB and TGBC* phases, XRD measurements were carried out for non-oriented samples **DC-4,11** and **DC-4,12**. The samples were filled into a Lindemann capillary (1 mm diameter) tube in the isotropic phase and both ends of the tube were flame sealed. The diffraction patterns obtained in the mesophase formed while cooling from the isotropic phase were collected on an image plate. As expected, the diffractograms obtained for the mesophase of both the compounds were qualitatively similar, and in fact evidenced the layer structure of TGB and TGBC* phases (for XRD patterns of dimers **DC-4**, and **DC-4,12**,

see Supporting Information). In the one-dimensional intensity versus 2θ profiles in the TGB and TGBC* phases at 117 and 100 °C for the dimer **DC-4,11**, it is seen that the diffraction pattern obtained for the TGB and TGBC* phase show a sharp reflection with *d* values of 47.26 and 44.31 Å, respectively, in the small-angle region. In addition, a diffuse peak is seen in the wide-angle region with *d* values of about 5 Å for both compounds, which can be attributed to the intermolecular separation within the layer arising due to the liquidlike positional correlation. The calculated length (*l*) in the most extended form in the all-trans configuration of the molecule **DC-4,11** measured using a Chem3D molecular model is 47 Å. Obviously, the *d* value of 46.7 Å in TGB phase suggests the blocks to be made of monolayer smectic A phase, and thus it is a TGBA phase. In the TGBC* phase, the layer spacing $d = 44.31$ Å TGBC* is, as expected, much less than the estimated all-trans molecular length, $l = 47$ Å, indicating the tilted organization of the molecules within the smectic layers with a tilt angle of $\sim 20^{o}$.

Summary

In this article, we have described the synthesis and thermotropic properties of new unsymmetrical dimers formed by combining a cholesteryl ester moiety covalently to a small size bent-core, namely, a chalcone unit through odd−even flexible alkylene central spacers. This investigation was undertaken with a view to enhance the chirality and to introduce the fluorescence property in cholesterol-based unsymmetrical dimers. Four homologues have been investigated with variation in the length and parity of the central flexible spacer. In each series, the length of alkoxy tail has been varied from ethoxy, *n*-butyloxy to *n*-dodecyloxy tails with the intention of understanding the structure and property relationship. In general, the majority of the dimers exhibit frustrated phase, especially the blue phase followed by the obvious short pitch chiral nematic phase, demonstrating that a small sized bent-core attached to cholesterol entity enhances the chirality of the system. The transition temperatures and phase behavior of unsymmetrical dimers belonging to three different series, in which two segments are separated by tri-, penta-, and hepta-methylene units, can be compared with each other to some extent. The dimers possessing a tetramethylene central spacer, as expected, exhibit low transition temperatures and in terms of phase behavior, the higher homologues of the series display interesting liquid crystal properties. Thus, the transitional behavior exhibits a dependence on the length and parity of the flexible spacer in a manner reminiscent of other reports. It can be seen that within the homologous series, the phase transition temperatures and the mesomorphic behavior, as anticipated, are dependent on the length of the alkoxy tail. In the homologous series of dimers having tri-, penta-, and hepta-methylene units, the clearing temperatures decrease as the length of alkoxy tail increases (with few exceptions), which can be attributed to enhancement in the flexibility of the systems. However, in the homologous series of dimers with tetramethylene spacer, for lower members with ethoxy and *n*-butyloxy tail the clearing temperature falls smoothly then begins to shift on the higher side for the dimers having pentyloxy, hexyloxy, and heptyloxy tail. Compounds with octyloxy and nonyloxy tail show a rapid increase in the clearing temperature, which then fall significantly for the dimers having decyloxy, undecyloxy, and dodecyloxy tails. Seemingly, in the context of liquid-crystal behavior within the homologous series, lower homologues exhibit BP and N* phases and the intermediate members stabilize TGB and/or SmA phase/s in addition, whereas several higher members (except for series II) display SmA behavior only. The stabilization of TGB and TGBC* phases over wide temperature range in a new phase sequence viz., I-TGB-TGBC* in dimers having tetramethylene spacer and decyloxy, undecyloxy, and dodecyloxy tails is remarkable.

Supporting Information Available: Detailed experimental procedures and molecular and liquid crystal property characterization data. This material is available free of charge via the Internet at http://pubs.acs.org.

CM0625880